Int. J. Heat Mass Transfer. Vol. 26, No. 5, pp. 671–679, 1983
Printed in Great Britain

0017-9310/83/050671 09 $03.00/0
Pergamon Press Ltd.

SIMPLIFIED NONLINEAR DESCRIPTIONS OF TWO-PHASE FLOW INSTABILITIES IN VERTICAL BOILING CHANNEL

H. GÜRGENCI,† T. N. VEZIROĞLU and S. KAKAÇ

Department of Mechanical Engineering, University of Miami, Coral Gables, FL 33124, U.S.A.

(*Received* 28 *June* 1982 *and in revised form* 27 *July* 1982)

Abstract—A constant-property homogeneous-flow model is developed to generate the limit cycles of pressure-drop and density-wave oscillations in a single-channel upflow boiling system operating between constant pressures, with upstream compressibility introduced through a surge tank. In the model, thermodynamic equilibrium conditions are assumed and the effects of the wall heat storage and the variation of the fluid properties are neglected. Satisfactory agreement with the experimental cycles is noted for the pressure-drop oscillations. As for the density-wave oscillations, the agreement with the experiments is reasonably good regarding the periods of the oscillations, but not so good for the amplitudes.

NOMENCLATURE

A, area;
C_t, dimensionless surge tank constant, $\rho_o L_h^3 A / p_{tas} V_{cs} \theta_s^2$;
d, diameter;
d_e, equivalent diameter;
F_M, two-phase friction multiplier;
f, friction factor;
G, mass flux;
$G(s)$, inlet flow-to-pressure drop transfer function;
g, gravitational acceleration;
h, enthalpy;
K_i, throttling constant between supply and surge tanks;
K_e, exit restriction pressure drop coefficient;
K_o, throttling constant between surge tank and heater;
L_i, length of tubing between supply and surge tank;
L_o, length of tubing between surge tank and heater inlet;
L_1, length of subcooled region;
p, pressure;
p_i, supply tank pressure;
p_e, system exit pressure;
p_t, surge tank pressure;
p_v, saturation pressure;
q', heat input per unit length;
s, complex variable;
T, temperature;
t, time;
t_1, residence time of a fluid particle in subcooled region;
t_2, residence time of a fluid particle in boiling heater region;
t_3, residence time of a fluid particle in exit tubing;
$U_o(s)$, Laplace transform of inlet velocity perturbation;
u, velocity;
V, volume;
V_c, surge tank compressible volume;
v, specific volume;
x, quality;
z, distance from heater inlet.

Greek symbols
ψ, system pressure drop;
ρ, density;
θ, reference time, $Ah_{fg}/v_{fg}q'_s$.

Subscripts
a, air;
b, incipient boiling point;
e, system exit;
f, saturated liquid;
g, saturated vapor;
i, surge tank inlet;
o, surge tank exit;
s, steady-state;
t, surge tank.

† On leave from the Middle East Technical University, Ankara, Turkey.

1. INTRODUCTION

THE TWO-PHASE flow instability problem can be approached in two ways: one may either work with the nonlinear conservation equations, solve them for certain initial conditions and see whether the solutions are asymptotically stable or not, or one may first linearize the governing equations and then analyze the resulting set of the linearized equations by well-tried linearized stability tests. Most of the two-phase flow instability studies published in recent years use linearized models to predict the instability thresholds and to generate stability maps for a given system. The linearized stability criteria are simpler to use, though the derivation of the criteria might be complicated. The effects of various physical parameters on stability are readily evident. However, for certain two-phase flow applications, the unstable operation may be the normal mode of operation, the frequencies and amplitudes being required to lie within specified limits. Then, linearized methods are of little use since they cannot provide information regarding the oscillation limit cycles. In such cases, solutions to the nonlinear equations are needed which, in most practical cases, can only be obtained by numerical means.

The development of new numerical codes for various two-phase flow applications has progressed in parallel with the advances in digital computer technology in the last two decades. One of the first successful attempts in this direction is by Meyer and Rose [1]. Since then, a multitude of computer codes have been developed and put into use in a diversity of industrial two-phase flow applications, such as the operation characteristics of an array of parallel channels (e.g. BWR bundles or steam generator tubes), steam condensation instabilities in BWR suppression pools, loss-of-coolant-accident (LOCA) processes in PWRs, countercurrent two-phase flow phenomena encountered in certain operation phases of PWRs and BWRs. A review of various computer codes developed by the national laboratories and private companies is given by Bouré [2]. Probably the best of them are proprietary.

An inherent problem of these nonlinear finite-difference solution schemes is that they are usually more useful for forecasting the system behavior under prescribed operating conditions than for parametric studies. The effects of changing various parameters on the subsequent behavior of the system are not readily evident. In order to achieve this purpose, a sufficient number of computer runs, or so-called 'numerical experiments', have to be performed, which may be time-consuming and prohibitively expensive in most cases.

In this study, two very simple numerical methods will be developed to simulate pressure-drop and density-wave oscillations in a single-channel upflow boiling system operating between constant pressures, with upstream compressibility introduced through a surge tank. The pressure-drop and the density-wave oscillations constitute two major types of two-phase flow instabilities. This terminology has been first proposed by Stenning and Veziroğlu [3] and it has been generally accepted.

A homogeneous equilibrium model will be developed in which the effects of the wall heat storage and the variation of the fluid properties are neglected. For the purposes of analyzing the density-wave oscillations, the system pressure drop is assumed to be concentrated at the two restrictions placed before and after the heater. The distributed pressure drop terms are included in the treatment of the pressure-drop oscillations, while, in this case, quasi steady-state conditions are assumed to persist throughout the system. The theoretical cycles will be compared with experimental cycles recorded on a single-channel vertical boiling flow system.

2. GOVERNING EQUATIONS

A schematic view of the upward-flow boiling system is represented in Fig. 1. A detailed description of the loop is given in ref. [4]. The governing equations for this system can be written as follows [5]:

Pressure-drop characteristics of the section between the supply and the surge tanks are given as

$$p_i - p_t = K_i \rho_o u_i^n + \rho_o L_i \frac{du_i}{dt} \tag{1}$$

where n is taken as 2 and K_i depends on the valve opening.

The time rate of change of the surge tank pressure is written as

$$\frac{dp_t}{dt} = \frac{(p_t - p_v)^2 A}{p_{tas} V_{cs}} (u_i - u_o) \tag{2}$$

where p_{tas} and V_{cs} are the steady-state values of the air partial pressure and the compressible volume in the surge tank, respectively. Assuming that the air–vapor mixture behaves ideally, $p_{tas} V_{cs}$ depends only on the mass of air trapped in the surge tank and the fluid inlet temperature.

Pressure drop after the surge tank:

$$p_t - p_e = \psi_{(u_o, \dot{u}_o, q')} \tag{3}$$

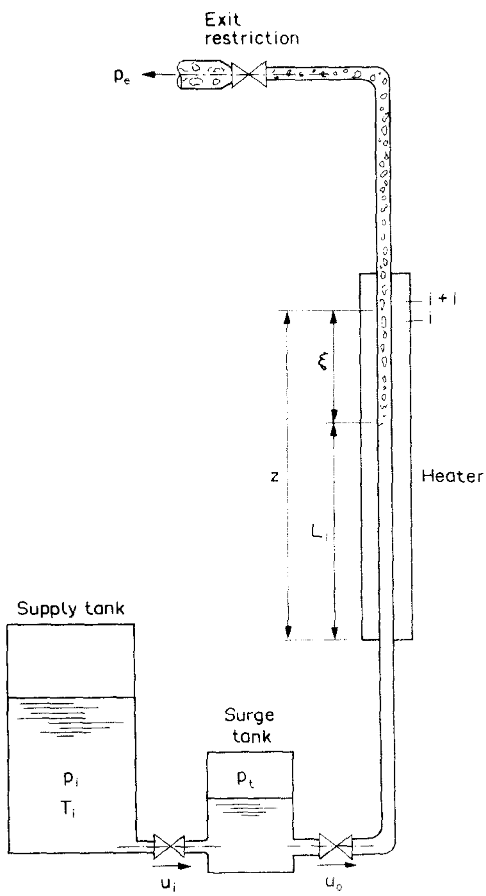

FIG. 1. Schematic diagram of the boiling upward-flow system.

where the specific form of the function, ψ, will be found by using a constant-property homogeneous-flow model.

The equations (1)–(3) govern the system behavior during steady-state and oscillatory flows. The boundary conditions on the system are prescribed as

$$p_i = \text{constant} \tag{4}$$

and

$$p_e = \text{constant}. \tag{5}$$

In the homogeneous flow model, conditions of thermodynamic equilibrium are assumed and the effects of the wall heat storage and the variation of fluid properties are neglected. With these assumptions, the mass and energy conservation equations for the homogeneous-flow model can be transformed into the following pair of dimensionless equations [5]:

$$\frac{\partial \bar{u}}{\partial \bar{z}} = \frac{1}{\bar{\theta}}, \tag{6}$$

$$\frac{1}{\bar{\rho}}\left[\frac{\partial \bar{\rho}}{\partial \bar{t}} + \bar{u}\frac{\partial \bar{\rho}}{\partial \bar{z}}\right] = -\frac{1}{\bar{\theta}}, \tag{7}$$

and the momentum equation is written as

$$\frac{\partial \bar{p}}{\partial \bar{z}} = -\bar{\rho}\frac{\partial \bar{u}}{\partial \bar{t}} - \bar{\rho}\bar{u}\frac{\partial \bar{u}}{\partial \bar{z}} - 2\frac{f}{d}\bar{\rho}\bar{u}^2 - \bar{\rho}\bar{g} \tag{8}$$

where the dimensionless variables are defined as follows:

$$\bar{z} = z/L_h;\quad \bar{t} = t/\theta_s;\quad \bar{\rho} = \rho/\rho_o;\quad \bar{u} = u\theta_s/L_h;$$
$$\bar{p} = p\theta_s^2/\rho_o L_h^2;\quad \bar{g} = g\theta_s^2/L_h;\quad \bar{\theta} = \theta/\theta_s. \tag{9}$$

The reference time, θ, is defined as

$$\theta \to \infty \qquad \text{when } h \leqslant h_f$$
$$\theta = A h_{fg}/v_{fg} q' \qquad \text{when } h_f < h \leqslant h_g. \tag{10}$$

Since the heat capacity of the wall is neglected, the heat input does not vary with time so that $\bar{\theta} = \theta/\theta_s = 1$ in the above equations. The two-phase friction factor, f, is assumed to be constant along the channel and equal to the liquid-phase friction factor in the subcooled region.

The equations (6) and (7) give the density and the velocity distribution along the system while equation (8) can be integrated to give the boundary condition on equations (6) and (7). The singular pressure drop across the exit restriction is given by

$$\Delta\bar{p}_{e(t)} = F_{M(x_e)} K_e \bar{G}_e^2 \tag{11}$$

where F_M is a two-phase friction multiplier which may be expressed as

$$F_M = c_1 x_e^2 + c_2 x_e + 1 \tag{12}$$

where the coefficients have been computed from the experimental data as $c_1 = 121$ and $c_2 = 30$.

3. PRESSURE-DROP OSCILLATIONS

The periods of the pressure-drop oscillations are very large compared with the residence time of a fluid particle through the system. Therefore, quasi steady-state conditions can be assumed along the test section. Then, one can write

$$\bar{\rho}_{(z,t)}\bar{u}_{(z,t)} = \bar{\rho}_o \bar{u}_{o(t)} = \bar{u}_{o(t)}. \tag{13}$$

Substituting this into equation (8) and performing the integration, the dimensionless time-dependent pressure drop across the system from the surge tank up to the exit is found as

$$\begin{aligned} p_t - p_e &= \psi_{[u_{o(t)}]} \\ &= \frac{2f_o u_o^2}{d}\left[L_o + \frac{t_1 u_o d}{d_e} + \frac{u_o d}{2d_e}\left(\frac{1}{u_o} - t_1\right)\right. \\ &\quad \left. \times\left(\frac{1}{u_o} - t_1 + 2\right) + L_e\left(\frac{1}{u_o} - t_1 + 1\right)\right] \\ &\quad + g\left[L_{oz} + t_1 u_o + u_o \ln\left(\frac{1}{u_o} - t_1 + 1\right)\right. \\ &\quad \left. + L_e\left(\frac{1}{u_o} - t_1 + 1\right)^{-1}\right] + u_o^2\left(\frac{1}{u_o} - t_1\right) \\ &\quad + [K_o + K_e F_{M(u_o)}]\, u_o^2 \end{aligned} \tag{14}$$

where the bars indicating non-dimensionality have been dropped for convenience. The quasi steady-state conditions have been assumed to prevail throughout the system and the inertial pressure drop terms have been neglected. This equation is applicable for $0 \leqslant x_e \leqslant 1$ or $1/t_1 \geqslant u_o \geqslant 1/(t_1 + v_{fg})$ since

$$x_e = (1/\rho_e - 1)/v_{fg} \tag{15}$$

or, assuming quasi steady-state conditions,

$$x_e = (1/u_o - t_1)/v_{fg}. \tag{16}$$

When u_o is greater or equal to $1/t_1$, the flow is single-phase throughout and the system pressure drop in this case is given by

$$\psi[u_{o(t)}] = 2\frac{f_o}{d}u_o^2\left(L_o + \frac{d}{d_e} + L_e\right) + g(L_{oz} + 1 + L_{ez}) + (K_o + K_e)u_o^2. \tag{17}$$

The surge tank pressure, p_t, is related to the surge tank inlet and outlet flow rates as given by the dimensionless form of equation (2),

$$\frac{dp_t}{dt} = C_t(p_t - p_v)^2(u_i - u_o) \tag{18}$$

where C_t is a dimensionless constant defined as

$$C_t = \frac{\rho_o L_h^3 A}{p_{tas} V_{cs} \theta_s^2}. \tag{19}$$

The mass flow rate at the surge tank entrance can be assumed to stay constant during the oscillations. This assumption is based on the fact that the pressure drop-flow rate characteristics of the section between the supply and the surge tanks are very stiff in comparison to the other parts of the system. During the experiments, it was observed that the surge tank inlet velocity, u_i, would not oscillate beyond $\pm 5\%$ of its nominal value even during the most violent oscillations. Therefore, equation (18) can be rewritten, by substituting

$$u_i = u_{os} \tag{20}$$

as

$$\frac{dp_t}{dt} = C_t(p_t - p_v)^2(u_{os} - u_o). \tag{21}$$

This is the governing equation for the pressure-drop oscillations. To examine the behavior of a particular steady-state operating point, the inlet velocity, u_{os}, is given a small perturbation supplying the initial condition for equation (21) as

$$u_o = u_{os} + \varepsilon, \quad \text{at } t = 0. \tag{22}$$

The solution will revert to the steady-state operating point if the system is stable at that point. Otherwise, sustained oscillations will be attained after a short transient. A simple finite-difference scheme to obtain the time-dependent solution is constructed as follows.

3.1. *Finite-difference solution scheme*

The surge tank pressure function, $p_{t(t)}$, at the time step $j+1$ is related to the value at the previous time step by

$$p_t^{j+1} = p_t^j + \Delta t C_t(p_t^j - p_v)^2(u_{os} - u_o^j) \tag{23}$$

and the heater inlet velocity is given in implicit form by

$$p_t^{j+1} - p_e = \psi(u_o^{j+1}) \tag{24}$$

where either equation (14) or equation (17) should be used for ψ, corresponding to the value of the exit quality. There is a slight problem here. The system pressure drop, $\psi(u_o)$, as given by equations (14) and (17), is a multi-valued function of the inlet velocity, u_o, for certain points when $\psi_{min} \leqslant \psi \leqslant \psi_{max}$, where the limits are the lower and the upper peaks of the pressure dropflow rate curve. Thus, for these points, there are three possible values for u_o^{j+1} at each time step, all of which satisfy equation (24). However, due to the inertia of the fluid volume inside the system, it is reasonable to expect the flow to follow a path of least resistance and to proceed to that value of u_o^{j+1} which is nearest to the one at the previous time step. In other words, at each time step $j+1$, out of all possible solutions for u_o^{j+1} given implicitly by equation (24), that value is chosen for which $|u_o^{j+1} - u_o^j|$ is minimum.

It should be noted that, in those parts of the solution domain, where the pressure function, ψ, increases or decreases monotonously, a simpler way of doing things is introduced as follows. Both equations (14) and (17) describe differentiable functions and it is trivial to obtain

$$\psi'_{(u_o)} \equiv d\psi/du_o \tag{25}$$

so that

$$dp_t/dt = \psi' \, du_o/dt \tag{26}$$

and equation (21) can be rewritten as

$$\frac{du_o}{dt} = C_t \frac{(p_t - p_v)^2}{\psi'} (u_{os} - u_o). \tag{27}$$

Then a simple finite-difference scheme is constructed as follows:

$$u_o^{j+1} = u_o^j + C_t(\Delta t)\frac{(p_t^j - p_v)^2}{\psi'(u_o^j)}(u_{os} - u_o^j) \tag{28}$$

and

$$p_t^{j+1} = \psi(u_o^{j+1}). \tag{29}$$

At each time step, compute

$$A \equiv (p_t^{j+1} - p_t^j)/\Delta t \tag{30}$$

and

$$B \equiv (dp_t/dt)^j = C_t(p_t^j - p_v)^2(u_{os} - u_o^j). \tag{31}$$

When A and B are of the same sign, the solution proceeds to the next time step through equation (28). When A and B are of opposite signs, the flow undergoes an excursion to another flow rate at the same pressure as governed by equation (24). It should be noted that this scheme is essentially the same as the first one, only more convenient because it is not necessary to solve u_o^{j+1} at each time step from the implicit relation of equation (24). An implicit iterative scheme for the velocity is sought for only immediately after the flow excursions.

3.2. *Results*

When the preceding finite-difference scheme is applied at different steady-state operating points, the subsequent behavior of the solution turns out to be in agreement with the predictions of the linearized analysis [5]. Those points for which the steady-state pressure drop increases with increasing flow rate have been found to be stable, the solution in such points reverts to steady-state conditions after a short transient. But when the starting point is in that part of the pressure drop-flow rate curve when the slope is negative, the initial perturbation slowly grows in size and leads to sustained pressure-drop oscillations.

A comparison with the experimental results is shown in Fig. 2. As seen from that figure, there is a fairly good agreement between the experimentally obtained and theoretically predicted amplitudes of the oscillations. However, the predicted periods are twice as long as the experimental periods. The main reason for this discrepancy between the experimental and theoretical periods is considered to be the way the flow excursions are treated. In the present model, it is assumed that the flow excursions occur instantaneously and at constant pressure. With a better explanation for the mechanism of flow excursions, it should be possible to get a fairly good agreement between the experimental and theoretical frequencies even with as simple a model as the present one.

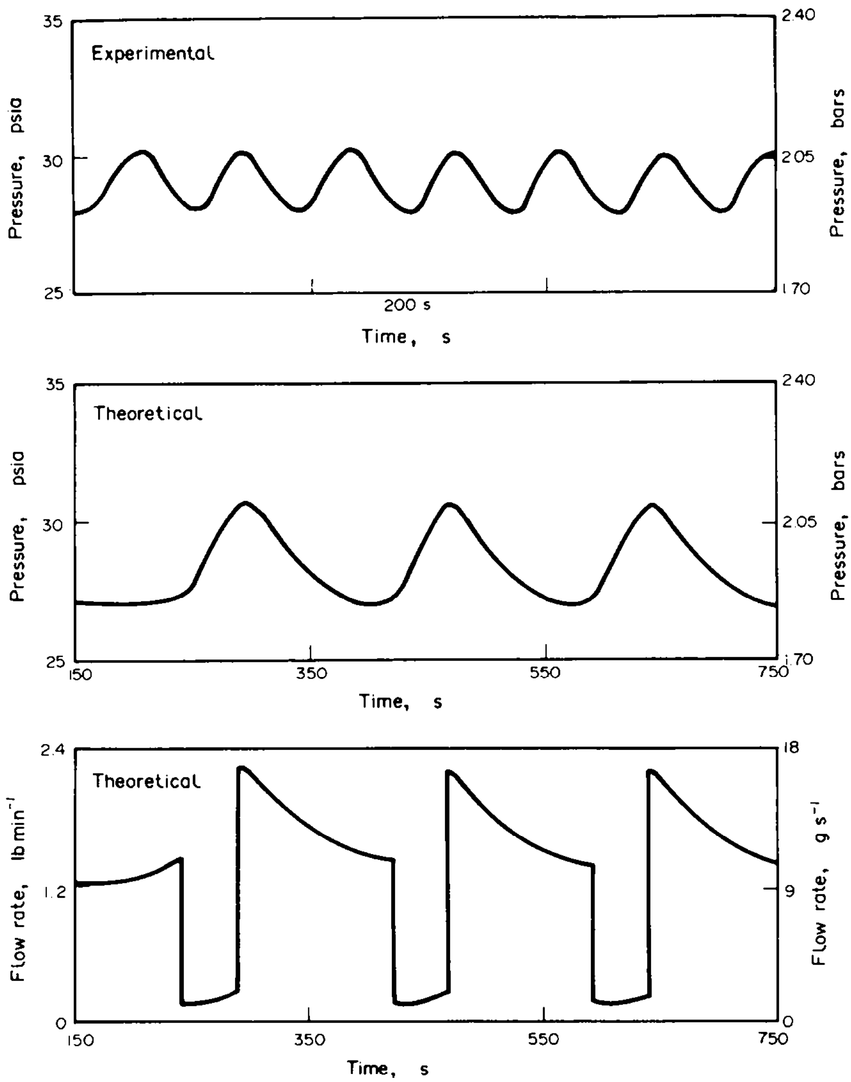

FIG. 2. Pressure-drop oscillations at $\dot{m} = 9.0\ \mathrm{g\ s^{-1}}$, $q = 300$ W, $T_i = 23°\mathrm{C}$, $m_a = 1.0$ g. Comparison between experimental cycles and results of homogeneous-flow model.

4. DENSITY-WAVE OSCILLATIONS

The density-wave oscillations have periods in the order of the residence time of a fluid particle in the heater. They are generated by the operation of complicated feedback mechanisms between the test section pressure drop and the fluid velocity. What is meant by the test section pressure drop is the pressure drop before and across the heater, across the exit tubing and the exit restriction. In order to simplify the analysis, this pressure drop will be assumed to be concentrated at two restrictions placed just before and after the heater. The system then consists of an inlet restriction, a heater tube where the fluid density changes through boiling and an exit restriction after the heater. The inlet and exit restrictions are represented by the throttling coefficients K_0 and K_e, respectively. The heater and the exit restriction are the essential components of the nonlinear time-delay feedback system which generate the density-wave oscillations. The inlet restriction has a stabilizing effect on these oscillations. A schematic view of the system after these simplifications is presented in Fig. 3.

The pressure at the incipient bulk boiling point, $p_b(t)$, is given by the following relation:

$$p_b = p_t - K_0 u_0^2 = K_e F_{M(x_e)} G_e^2 + p_e \tag{32}$$

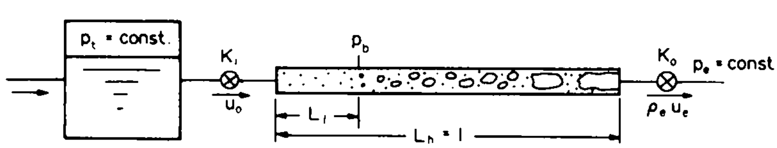

FIG. 3. Simplified system diagram for density-wave oscillations.

where the two-phase friction multiplier is defined as

$$F_{M(x_e)} = c_1 x_e^2 + c_2 x_e + 1 \quad (33)$$

where c_1 and c_2 are constants and the quality is related to the exit density by

$$x_e = (1/\rho_e - 1)/v_{fg}. \quad (34)$$

Integrating equation (7), the following implicit relation for the exit density, ρ_e, is obtained:

$$1 = e^t \int_{t+\ln\rho_e}^{t} u_{o(t-t_1)}\, e^{-t}\, dt + L_{1(t)} \quad (35)$$

and the subcooled length, $L_{1(t)}$, is given by

$$L_{1(t)} = \int_{t-t_1}^{t} u_{o(t)}\, dt \quad (36)$$

where the time lag, t_1, is defined as

$$t_1 = \rho_o v_{fg}(h_f - h_i)/h_{fg} \quad (37)$$

which represents the dimensionless residence time of a fluid particle in the subcooled region of the heater.

The mass flux through the exit restriction, $G_{e(t)}$, is defined as

$$G_e = \rho_e u_e = \rho_e(u_o - L_1 + 1). \quad (38)$$

The surge tank pressure, p_t, will be assumed to be constant in the analysis. This assumption is in close agreement with the experimental observations where the high-frequency density-wave oscillations are easily absorbed by the inertia of the surge tank volume.

The two governing equations (one forward and one feedback relation) for the density-wave oscillations are written from equation (32) as

$$p_b = K_e F_{M(x_e)} G_e^2 + p_e \quad (39)$$

and

$$u_o = \left(\frac{p_t - p_b}{K_o}\right)^{1/2}. \quad (40)$$

As in the previous section on the pressure-drop oscillations, to examine the behavior of a particular steady-state operating point, the inlet velocity at that point, u_{os}, will be given a small perturbation at time, $t = 0$,

$$u_o = u_{os} + \varepsilon, \quad \text{at } t = 0. \quad (41)$$

This will be the initial condition for equations (39) and (40). As time progresses, the solution will either revert to the steady-state operating point, if the system is stable at that point, or sustained oscillations will be achieved after a short transient. A simple finite-difference scheme to obtain the time-dependent solution is constructed as follows.

4.1. *Finite-difference solution scheme*

The pressure, p_b, at the $(j+1)$th time step is given by

$$p_b^{j+1} = K_e F_{M(x_e^{j+1})}(G_e^{j+1})^2 + p_e \quad (42)$$

where the quality is to be calculated from

$$x_e^{j+1} = (1/\rho_e^{j+1} - 1)/v_{fg}. \quad (43)$$

The time rate of change of the exit density may be obtained from equation (35) as

$$\frac{d\rho_{e(t)}}{dt} = \rho_{e(t)}\left[\frac{\rho_{e(t)} u_{e(t)}}{u_{o(t-t_1+\ln\rho_e)}} - 1\right] \quad (44)$$

so that

$$\rho_e^{j+1} = \rho_e^j + \Delta t \rho_e^j \left[\frac{\rho_e^j u_e^j}{u_o^{j-n}} - 1\right] \quad (45)$$

where

$$n = \left[\!\left[\frac{t - t_1 + \ln\rho_e}{\Delta t}\right]\!\right] \quad (46)$$

and the open brackets indicate the integer operator.

Similarly, equation (36) yields

$$\frac{dL_{1(t)}}{dt} = u_{o(t)} - u_{o(t-t_1)} \quad (47)$$

so that

$$L_1^{j+1} = L_1^j + \Delta t[u_o^j - u_o^{j-m}] \quad (48)$$

where

$$m = [\![(t - t_1)/\Delta t]\!] \quad (49)$$

and G_e^{j+1} is to be found from

$$G_e^{j+1} = \rho_e^{j+1} u_e^{j+1}. \quad (50)$$

A simple algorithm to generate the solution may be stated as follows:

(1) Compute L_1^{j+1} from equation (48).
(2) Compute ρ_e^{j+1} from equation (45).
(3) Compute x_e^{j+1} from equation (43).
(4) Use the following predictor formula for u_e^{j+1}:

$$(u_e^{j+1})^p = 2u_e^j - u_e^{j-1}. \quad (51)$$

(5) Compute G_e^{j+1} from equation (50).
(6) Compute p_b^{j+1} from equation (42).
(7) Compute u_o^{j+1} from the following:

$$u_o^{j+1} = \left[\frac{p_t - p_b^{j+1}}{K_o}\right]^{1/2}. \quad (52)$$

Reverse flow is not allowed so that $u_o^{j+1} = 0$ for $p_t < p_b^{j+1}$.

(8) Compute $(u_e^{j+1})^c$ from the following:

$$(u_e^{j+1})^c = u_o^{j+1} - L_1^{j+1} + 1. \quad (53)$$

(9) If $(u_e^{j+1})^c \cong (u_e^{j+1})^p$, go to the next step. Otherwise, correct $(u_e^{j+1})^p$ and return to the 5th step. The corrector formula is

$$(u_e^p)^{\text{new}} = (u_e^p)^{\text{old}} + 0.1[u_e^c - (u_e^p)^{\text{old}}]. \quad (54)$$

(10) Go to the next time increment and start from the first step.

4.2. *Results*

The algorithm explained in the preceding section has been applied at different steady-state operating points. The limit cycles for the density-wave oscillations have been obtained at various heat input and mass flow rate values. A typical example of experimental density-wave oscillation cycles is presented in Fig. 5. The predicted cycles at the same operating point are shown in Fig. 4. As seen from this figure, the frequency of the theoretical cycles is about 5 cps which is in good agreement with the experimental frequencies (4–6 cps). However, the amplitudes of the theoretical cycles are bigger than the actual experimental amplitudes. From Fig. 4, it is observed that the heater inlet pressure apparently drops as low as the system exit pressure during the theoretical cycles. This is due to the fact that the system pressure drop is assumed to be concentrated at two restrictions. Thus, when the flow is blocked at the exit orifice as happens during a cycle, the pressure drop after the heater inlet simply vanishes according to the model. Actually, a part of the system pressure drop is distributed along the heater and the exit tubing. This pressure drop, which is composed of frictional, gravitational, accelerational and inertial components, is never zero; therefore, the lower limit for the actual heater inlet pressure cycles is higher than the one predicted by this analysis. However, when compared with the more elaborate models of the previous studies [7, 8], the results of the present simplified model seem to be equally reasonable. The model can be improved by considering a distributed pressure drop across the system, instead of the present singularities. This would require a few additional manipulations during the numerical computations but the final results would be more realistic.

5. CONCLUSIONS

A constant-property homogeneous equilibrium model was developed to generate the limit cycles of pressure-drop and density-wave oscillations in a single-channel upflow boiling system operating between constant pressures, with upstream compressibility introduced through a surge tank. Thermodynamic equilibrium conditions were assumed and the effects of the wall heat storage were neglected. For the density-wave oscillations, the system pressure drop was assumed to be concentrated at two restrictions placed before and after the heater. The distributed pressure drop terms were included in the treatment of the pressure-drop oscillations, while, in this case, quasi steady-state conditions were assumed to persist throughout the system.

Regarding the pressure-drop oscillations, there is a fairly good agreement between the experimental and the theoretical cycles. The discrepancy in the periods is presumably due to the incomplete description of the

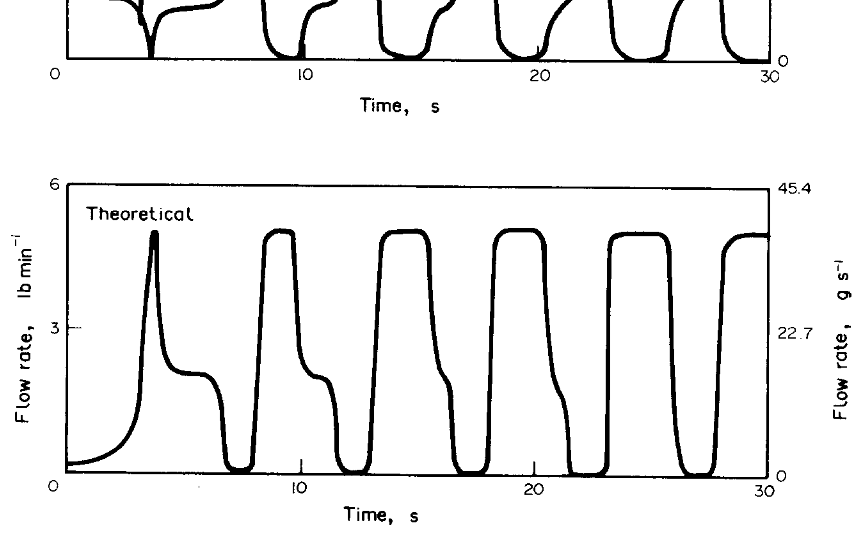

FIG. 4. Development of density-wave oscillation cycles as predicted by homogeneous-flow model ($\dot{m} = 1.5$ g s^{-1}, $q = 350$ W, $T_i = 23$°C).

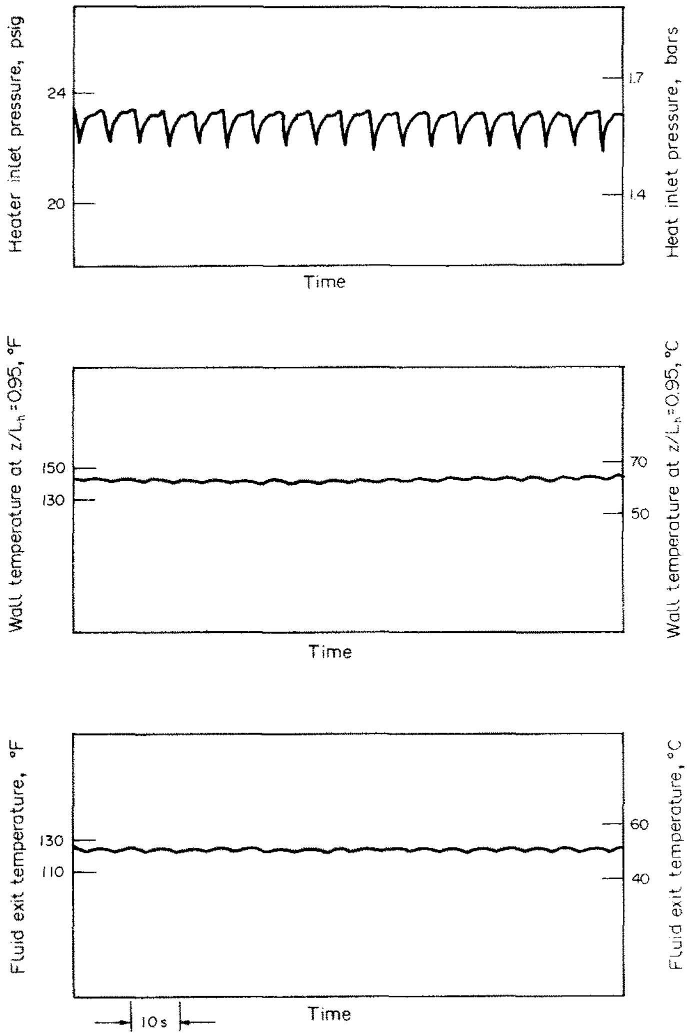

FIG. 5. Experimental density-wave oscillation cycles ($\dot{m}$ = 1.5 g s^{-1}, q = 350 W, T_i = 23°C).

flow excursions which play an important role in the pressure-drop oscillations.

As for the density-wave oscillations, the theoretical frequencies are in good agreement with the experimental frequencies. However, the amplitudes differ, which fact is basically due to neglecting the distributed pressure drops along the system.

The proposed solution scheme is very easy to apply on a digital computer and little computer time is required. The effects of various factors on the amplitudes and the frequencies of the oscillations are readily evident due to the simplicity of the model. The model is especially useful for parametrical studies to clarify the basic nonlinear mechanisms of the oscillations, without using too much computer time.

Acknowledgements—The authors gratefully acknowledge the financial support of the National Science Foundation. The authors extend their thanks to A. Menteş and O. T. Yildirim for their very valuable suggestions. The secretarial work of Ms. Norma Sage is also acknowledged.

REFERENCES

1. J. Meyer and R. Rose, Application of a momentum integral model to the study of parallel channel boiling flow oscillations, *J. Heat Transfer* **85**, 1 (1963).
2. J. A. Bouré, A. E. Bergles and L. S. Tong, Review of two-phase flow instability, *Nucl. Engng Des.* **25**, 165 (1973).
3. A. H. Stenning and T. N. Veziroğlu, Flow oscillation modes in forced convection boiling, *Proc.* 1965 *Heat Transfer and Fluid Mechanics Institute*, pp. 301–316, Stanford University Press, Stanford, California (1965).
4. A. Menteş, H. Gürgenci, O. T. Yildirim, S. Kakaç and T. N. Veziroğlu, Effect of heater surface configurations on two-phase flow instabilities in a vertical boiling channel, *Proc.* 16*th Southeastern Seminar on Thermal Sciences*, 19–21 April, Miami, Florida (1982).
5. H. Gürgenci, Two-phase flow instabilities, Ph.D. Thesis, University of Miami, Coral Gables, Florida (1982).
6. T. N. Veziroğlu and S. Kakaç, Two-phase flow instabilities, NSF Project ME 79-20018, Final Report (1982).
7. K. Akyüzlü, T. N. Veziroğlu, S. Kakaç and T. Doğan, Finite difference analysis of two-phase pressure-drop and density-wave oscillations, *Wärme- und Stoffübertragung* **14**, 253–267 (1980).
8. T. N. Veziroğlu and S. Kakaç, Two-phase flow instabilities and effect of inlet subcooling, NSF Project Eng 75-16618, Final Report (1980).

DESCRIPTIONS SIMPLIFIEES NON LINEAIRE DES INSTABILITES D'UN ECOULEMENT DIPHASIQUE DANS UN CANAL VERTICAL AVEC EBULLITION

Résumé—On établit un modèle d'écoulement homogène à propriétés constantes pour obtenir les cycles limites des oscillations de pression et d'onde de densité dans un écoulement ascendant en ébullition, avec compressibilité en aval introduite par un réservoir. Dans le modèle, les conditions d'équilibre thermodynamique sont supposées et les effets de stockage thermique de la paroi et ceux de la variation des propriétés du fluide sont négligés. Un accord satisfaisant avec les cycles expérimentaux est noté pour les oscillations de chute de pression. En ce qui concerne les oscillations d'onde de densité, l'accord avec les expériences est raisonnable pour les périodes des oscillations, mais pas aussi bon pour les amplitudes.

VEREINFACHTE NICHTLINEARE BESCHREIBUNG VON INSTABILITÄTEN DER ZWEIPHASENSTRÖMUNG BEIM SIEDEN IN SENKRECHTEN KANÄLEN

Zusammenfassung—Unter Verwendung konstanter Stoffwerte wird ein Modell der homogenen Strömung entwickelt, um die Grenzfrequenzen der Schwingungen von Druckabfall und Dichtewellen einer siedenden Aufwärtsströmung in einem Einkanalsystem zu erhalten, welches zwischen konstanten Drücken arbeitet, wobei eine Kompressibilität in Strömungsrichtung durch einen Windkessel zustandekommt. Für das Modell wird thermodynamisches Gleichgewicht angenommen. Der Einfluß der Wärmespeicherung in der Wand sowie Änderungen der Stoffwerte des Fluids werden vernachlässigt. Gute Übereinstimmung mit den experimentell gefundenen Frequenzen wird bei den Schwingungen des Druckabfalls festgestellt. Bei den Dichtewellen-Schwingungen ist die Übereinstimmung befriedigend für die Perioden, nicht aber für die Amplituden der Schwingungen.

УПРОЩЕННОЕ НЕЛИНЕЙНОЕ ОПИСАНИЕ НЕУСТОЙЧИВЫХ ДВУХФАЗНЫХ ПОТОКОВ ПРИ КИПЕНИИ В ВЕРТИКАЛЬНОМ КАНАЛЕ

Аннотация—Разработана модель однородного течения с постоянными свойствами с целью определения пределов колебаний перепадов давления и волн плотности в единичном канале с восходящим кипящим потоком, в котором давление изменяется в диапазоне между двумя постоянными значениями. Предлагаемая модель предполагается термодинамически равновесной, а теплоотдача от стенок и изменение свойств жидкости считаются пренебрежимо малыми. Расчетные значения колебаний перепадов давления удовлетворительно согласуются с экспериментальными. Что касается колебаний волн плотности, то с экспериментальными данными достаточно хорошо согласуются расчетные значения периода колебаний и хуже — значения их амплитуд.